THERMOPHYSICAL PROPERTIES OF MOLTEN GERMANIUM MEASURED BY THE HIGH TEMPERATURE ELECTROSTATIC LEVITATOR

Won-Kyu Rhim and Takehiko Ishikawa*
Jet Propulsion Laboratory, California Institute of Technology,
4800 Oak Grove Drive, Pasadena, California 91109, USA

*On leave from the National Space Development Agency of Japan

ABSTRACT

Thermophysical properties of molten germanium such as the density, the thermal expansion coefficient, the hemispherical total emissivity, the constant pressure specific heat capacity, the surface tension, and the electrical resistivity have been measured using the High Temperature Electrostatic Levitator at JPL. The measured liquid density can be expressed by $\rho_{liq.} = 5.67 \times 10^3 - 0.542\ (T - T_m)$ Kg m^{-3} (1150 ~ 1400 K) with T_m = 1211.3 K, the volume expansion coefficient by $\alpha = 0.9656 \times 10^{-4}\ K^{-1}$, and the hemispherical total emissivity at the melting temperature by $\varepsilon_{T,liq}(T_m) = 0.17$. Assuming constant $\varepsilon_{T,liq}(T) = 0.17$ in the liquid range which have been investigated, the constant pressure specific heat was evaluated as a function of temperature (see Fig. 5 in the text). The surface tension over the same temperature range can be expressed by $\sigma(T) = 583 - 0.08\ (T - T_m)$ mN m^{-1} and the temperature dependence of electrical resistivity of molten germanium, when $r_{liq}(T_m) = 60$ $\mu\Omega$cm is used as a reference point, can be expressed by $r_{e,liq}(T) = 60 + 1.18 \times 10^{-2}\ (T - 1211.3)$ $\mu\Omega \cdot$cm. The thermal conductivity which is determined by the resistivity data according to the Wiedemann-Franz-Lorenz law is given by $\kappa_{liq}(T) = 49.43 + 2.90 \times 10^{-2}\ (T - T_m)$ W m^{-1} K^{-1}.

KEY WORDS: Electrostatic levitation; molten germanium; density; hemispherical total emissivity; specific heat; surface tension; electrical resistivity; thermal conductivity.

---

1. INTRODUCTION

Thermophysical properties of molten semiconductors are needed in understanding the liquid structures and the solidification process in general, and for the numerical modeling of crystal growth processes in particular. Although solid germanium has been rather extensively investigated, properties of molten germanium are rather scarce. Even then, of they exist, there are substantial differences among them.

In this paper, we revisit the molten germanium, this time with various non-contact methods, and report its properties such as the density, the volume expansion coefficient, the hemispherical total emissivity, the specific heat, the surface tension, and the temperature dependence of electrical resistivity. These properties have been measured using the High Temperature Electrostatic Levitator (HTESL) which isolated the samples from container walls during entire experiments in a high vacuum condition. Under such condition, the purity of samples could be maintained, highly undercooled liquid states are expected, and their properties can be measured using appropriate non-contact diagnostic techniques which have been developed for the HTESL.

The HTESL[**1**] at JPL can levitate conducting as well as semiconducting materials. Some of the characteristics of HTESL which made the present work possible are: (i) it can levitate a pure germanium sample one at a time, melt it while in levitation, and can reach an undercooled state when it is cooled, (ii) the sample heating and the levitation do not interfere each other so that the sample can be cooled in a purely radiative manner when the heating source was either turned off or blocked. This allowed description of the whole cooling process by a well defined heat transfer equation, allowing accurate measurement of c_p/ε_T. (iii) Levitated drop is quiescent and maintains nearly perfect spherical shape, simplifying the processes of accurately measuring the volume changes, the surface tension, and the viscosity. (iv) The system is equipped with a newly developed capability of measuring electrical resistivity by applying rotating magnetic field to a levitated sample. This capability has an additional implication for the indirect determination of thermal conductivity through the Wiedemann-Franz-Lorenz law, which relates the electrical resistivity with the thermal conductivity for certain metallic substances.

2. EXPERIMENTAL PROCEDURE

The HTESL levitates a sample 1 to 3 mm in diameter between a pair of parallel disk electrodes spaced about 12 mm apart (**Fig. 1**). In Fig. 1, the four small side electrodes around the bottom electrode control the sample position along horizontal direction, and the four coils positioned around the top electrode induce sample rotation. The electrode assembly is housed

by a stainless steel chamber which is typically evacuated to 10^{-8} Torr before sample heating begins. Samples are heated using a 1-KW xenon arc lamp. Detailed description of the HTESL is given in an earlier publication [1].

Once a levitated sample is molten, the melt shows very nearly spherical shape. In order to maintain clean surfaces during processing, it was necessary to begin with pure, clean samples. Germanium samples were prepared from 99.9999% pure stock from Johnson-Matthey. These were then ground roughly into spheres. They were cleaned by immersion in 5% hydrofluoric acid at room temperature for 5 minutes, rinsed in distilled water, and finally rinsed in anhydrous ethanol. The samples weighed approximately 20 mg.

Since the electrostatic levitation mechanism does not affect the sample temperature, a sample that is heated to a certain high temperature will cool purely radiatively when the heating source is blocked, and the ensuing cooling process can be described by the radiative heat transfer equation

$$mc_p \frac{dT}{dt} = -\sigma_{SB}\varepsilon_T A(T^4 - T_E^4), \qquad (1)$$

where m is sample mass, c_p is the constant pressure specific heat capacity, T is the sample temperature, T_E is the environment temperature, σ_{SB} is the Stefan-Boltzmann constant (5.6705×10^{-8} $W \cdot m^{-2} \cdot K^{-4}$), and ε_T is the hemispherical total emissivity. The fact that accurate measurement of c_p/ε_T is possible from Eq. (1) is one of the most important merits of the HTESL.

Measurements of the mass density and the specific heat capacity of molten germanium was initiated by blocking the heating source and allowing the germanium melt to cool until recalescence took place. Upon beam blocking, both the temperature measurement by a pyrometer and the image recording by a video system went on simultaneously throughout cooling process. A typical temperature versus time profile for a germanium melt obtained during such a cooling process is shown in **Fig. 2.** The melt started to cool from about 200 K above the melting temperature and undercooled approximately 60 K before recalescence took place. Upon recalescence the sample temperature rose sharply and reached isotherm state. It is interesting to note that, unlike the silicon case[2], **Fig. 2** shows constant spectral emissivity over the isotherm region. Output of the single color pyrometer operating at 750 nm was calibrated using Planck's spectral distribution of emissive power taking the temperature immediately following the recalescence as its melting temperature (T_m=1211 K). 750 nm spectral emissivity of the melt over the entire liquid temperature range was assumed to be constant.

Temperature dependence of the mass density was measured by analyzing the video images taken during a cooling process. The image size was extracted from each video frame using an image analysis method which was developed in our laboratory [3].

To measure the surface tension, a low amplitude drop excitation field pulse was applied along the vertical direction and the transient drop oscillation following the pulse was recorded in a computer for later analysis. The drop excitation was done by applying an electric field pulse which varies sinusoidally at the drop resonance frequency. When the drop oscillation is sufficiently low in amplitude, one can utilize the Rayleigh's formula to determine the surface tension from the measured resonance frequency[4].

The surface charge on a levitated drop lowers the apparent surface tension, and the drop oscillation frequency reflects this. If we know the net drop charge, one can use the Rayleigh's expression for charged drop oscillation to extract the true surface tension σ [5],

$$\omega = \left[\frac{8\sigma}{\rho r_o^3}\left(1 - \frac{Q^2}{16\pi r_o^3 \sigma}\right)\right]^{\frac{1}{2}}, \qquad (2)$$

where ω is the angular frequency of observed oscillation, ρ is the mass density of the melt, r_o is the radius of the melt when it is in spherical shape, and Q is the net sample charge. Effects on surface tension due to non-uniform charge distribution and deviation from a perfect spherical shape were corrected using the perturbation analysis of electrostatically levitated drops which was derived by Feng and Beard [6].

3. MEASUREMENTS OF THE DENSITY AND THE THERMAL EXPANSION COEFFICIENT

Thermophysical properties of molten materials are intimately related to its density. The method we used in this work is basically an image analysis technique. This method consisted of (i) digitization of recorded video image, (ii) edge detection, (iii) calculation of the area (therefore, the volume of the sample) through linear spherical harmonic fit, and (iv) calibration of data with respect to a reference sphere for absolute values. The density was then obtained using the sample mass which was measured immediately following the experiment. Detailed description of the image analysis method used in this experiment was published elsewhere [3].

Fig. 3 shows the result of our density measurements of molten germanium over the temperature of 250 K. Unlike the density of molten silicon which showed pronounced quadratic behavior [2], the density of molten germanium rather shows a linear behavior which can be expressed in the following form:

$$\rho_{liq.}(T) = \rho_{liq.}(T_m) + \frac{d\rho_{liq.}}{dT}(T - T_m) \quad \text{Kg/m}^3, \tag{3}$$

where the coefficients for the present result can be expressed by $\rho_{liq.}(T_m) = 5.67 \times 10^3$ Kg/m^3 and $d\rho_{liq.}/dT = -5.42 \times 10^{-1}$ Kg/Km^3. The Table I compares the present work with three other works which could be found in the literature. $\rho_{liq.}(T_m)$ obtained by Lucas[7] using the bubble pressure method and by other workers using the pycnometer and volumetric measurement methods are about 2.3 % smaller than the our result. On the other hand, the results obtained by sessile drop method by Khilya et al.[8] and also by Tavadse et al.[9] agree with the present work within 1.25 %.

However, our temperature dependence of density shows $(\frac{\partial \rho}{\partial T})_P = -5.42 \times 10^{-1}$ Kg/Km^3 which is 10 % larger than the Lucas's, while it is approximately 13 % smaller than those obtained by Khilya and Tavadse. Our result translates into the isobaric thermal expansivity $\alpha = 0.9656 \times 10^{-4}$ K^{-1} which is reasonably in good agreement with ~0.9 given by Iida[10].

4. SPECIFIC HEAT MEASUREMENT

Constant pressure specific heat capacity is a very important thermodynamic parameter from which other parameters, such as enthalpy, entropy, and Gibbs free energy can be derived. In spite of their importance, specific heat capacity and hemispherical total emissivity are known for very few high-temperature liquids. Data are particularly scarce for the undercooled liquids since they tend to solidify when placed in contact with most crucibles. The HTESL allows determination of c_p/ε_T in a simple heat transfer environment while the levitated melt cools to undercooled states. Rearrangement of Eq. (1) gives

$$\frac{c_p}{\varepsilon_T} = -\frac{\sigma_{SB} A (T^4 - T_E^4)}{m \frac{dT}{dt}}. \tag{4}$$

Using temperature-time profile obtained experimentally (as shown in **Fig. 2**), and evaluating dT/dt from it, c_{pl}/ε_T can be obtained as shown in **Fig. 4**. From this ratio $c_p(T)$ can be determined if $\varepsilon_T(T)$ is known, and conversely, $\varepsilon_T(T)$ can be found if $c_p(T)$ is known [11].

Frequently, specific heat values are known in many materials at their melting temperature, while the values for hemispherical total emissivity are not. In such cases, $\varepsilon_T(T_m)$ at the melting temperature can be obtained. The literature value of the constant pressure specific

heat capacity of molten germanium at the melting temperature is $C_{p,liq}(T_m)$ = 27.61 J/mol K[12]. With this value together with the c_{pl}/ε_T shown in **Fig. 4**, the hemispherical total emissivity at the melting temperature $\varepsilon_T(T_m)$ is determined to be 0.17. This is in good agreement with Brekhovskikh's prediction that $\varepsilon_T(T)$ for the liquid will not exceed 0.18[**13, 14**].

Strictly speaking, in order to evaluate $c_p(T)$, the temperature dependence of $\varepsilon_T(T)$ has to be independently measured. Since $\varepsilon_T(T)$ is not available at the present time, let us assume that it remains constant at $\varepsilon_T(T) = \varepsilon_T(T_m) = 0.17$ over the liquid region of present interest, and evaluate $c_p(T)$ from **Fig. 4**. Such assumption may be a reasonable one if we consider the fact that the spectral emissivities of molten germanium at both visible and infrared wavelengths show almost no temperature dependence[**15**]. **Fig. 5** shows $c_p(T)$ as a function of temperature so obtained. Like molten silicon[**2**], $c_p(T)$ of molten germanium also shows a non-linear behavior, decreasing with the increased temperature.

5. SURFACE TENSION

Spherical shape of a molten drop levitated by the HTESL greatly simplifies the surface tension measurements. In view of the fact that surface tension is particularly sensitive to even minute surface contamination, the high vacuum environment would be ideal for measuring surface tension, particularly of those chemically reactive materials.

For surface tension experiments we had to fix the sample temperature at a predetermined value until the surface tension data at that temperature was obtained. The pyrometer used for this experiment operated at 4 μm wavelength to avoid interference by the xenon arc-lamp radiation. As described in Section 2, a low amplitude electric pulse was applied along the vertical direction and the transient drop oscillation following the pulse was recorded in a computer. The electric field pulse has sinusoidal career frequency at the drop resonance frequency.

Fig. 6 shows our surface tension result on molten germanium as a function of temperature. The surface tension data can be expressed by

$$\sigma(T) = 583 - 0.08\,(T - T_m) \quad \text{mN/m.} \qquad (1160 \sim 1430\ \text{K}) \qquad (5)$$

The surface tension 583 $mN \cdot m^{-1}$ at the melting temperature is more than 6 % smaller than 621 $mN \cdot m^{-1}$ reported by Allen [**16**] and approximately 3 % smaller than the value recently reported by Takamura[**17**]. As for $d\sigma(T)/dT$, the present result shows 0.08 $mN \cdot m^{-1} \cdot K^{-1}$ while Ref. [**16**] and [**17**] showed 0.26 $mN \cdot m^{-1} \cdot K^{-1}$ and 0.16 $mN \cdot m^{-1} \cdot K^{-1}$, respectively. At the present

time, it is too premature to prefer a particular result over others. Our levitation method in vacuum supposed to expose cleaner surface, yet it is surprising that our result show smaller surface tension than the reference values. Only more comprehensive experimental conditions in each of different experimental approaches would be able to reveal causes of such different results.

If we measure the decay time constants of transient free oscillation signals, we should be able to relate them to the viscosity of the melt through the following relationship[**18**]

$$\frac{1}{\tau_2} = \frac{5\eta}{\rho r_o^2}. \qquad (6)$$

In Eq. (6), τ_2 is the time constant of exponentially decaying signal, η is the viscosity of the sample liquid, ρ is the density of the melt, and r_o is the radius of the drop. However, we discovered that the time constant we were measuring was highly sensitive to external perturbation forces. Such susceptibility to external noise is relatively more pronounced as the viscosity of the melt decreases. In the present case, the most dominant perturbing force was coming from the levitation force correcting the sample position 480 times per second. The viscosity data we obtained scattered between 0.13 mPascal·sec and 0.7 mPascal·sec. over the 1160 K ~ 1425 K range. In contrast, Glazov et al.[**19**] and Turovskii et al.[**20**] reported 0.78 mPascal·sec and 1.1 mPascal·sec for the viscosty at the melting point, respectively.

6. TEMPERATURE DEPENDENCE OF ELECTRICAL RESISTIVITY AND THERMAL CONDUCTIVITY

Electrical resistivity is known to be sensitive to reflect the state of local structures liquids. Utilizing the sample rotation capability which was newly built into the HTESL, the measurement of temperature dependence of electrical resistivity was attempted. To exert a torque to a levitated conducting sample, a rotating magnetic field was applied to the sample with its rotation axis coinciding with the gravitational field. The basic principle is same as the asynchronous motor in which the sample being investigated is the rotor. In fact, along with the four probe method, the rotating magnetic field method[**10**] is frequently used to measure electrical conductivity of molten material. Only difference between this method and our method is in the necessity of container which holds the sample liquid. The sample rotation method which can measure the electrical resistivity (or conductivity) of a molten sample which is levitated in a high vacuum by the HTESL is truly a non-contact method.

According to the principle of induction motor[**21, 22**], the torque τ is given by

$$\tau \propto \frac{s r_e}{r_e^2 + s^2 X^2}, \tag{7}$$

where

$$s \equiv \frac{\omega_s - \omega}{\omega_s}, \tag{8}$$

r_e is the electrical resistance of the rotor at a given temperature (the sample in the present case), X is the inductive reactance of the rotor, ω_s is the angular frequency of applied field, and ω is the instantaneous rotation frequency of the rotor. To make the Eq. (7) useful for the resistivity measurements, it is important to keep the amplitude of applied magnetic field experienced by the rotor stay constant for a given ω_s throughout a resistivity measurement. In the present experiment on molten germanium, the condition $r_e^2 >> s^2X^2$ was satisfied to make the Eq. (7) even simpler, i.e.

$$\tau \propto \frac{1}{r_e}\left(\frac{\omega_s - \omega}{\omega_s}\right) \tag{9}$$

Once the validity of Eq. (9) was experimentally verified using a molten aluminum drop, the resistivity of molten germanium was determined by measuring the torque of a levitated sample in the neighborhood of $\omega = 0$. Detailed description of this technique will be published elsewhere [23].

Since our intent is to measure the relative electrical resistivity of molten germanium over a certain temperature range, it requires a reference value at a known temperature. Keyes[24] reported $r_{e,liq}(T_m) = 0.6\ \mu\Omega m$, while 0.63 $\mu\Omega m$ was reported by Domenicali[25], and 0.6 $\mu\Omega m$ by Glazov[18]. If we choose $r_{e,liq}(T_m) = 0.6\ \mu\Omega m$ to calibrate our data, the our measured data can be expressed by the following equation:

$$r_{e,liq}(T) = 0.6 + 1.18 \times 10^{-4}\,(T-1211.3)\ \mu\Omega m. \qquad (1211.3 \sim 1380\ K) \tag{10}$$

Fig. 7 shows our result along with the Glazov's work. While our data nicely fall onto a simple line, Glazov's data seem to show a rather complex structure. Whether such a structure has a physical meaning or it is simply an expression of uncertainties involved in his experiment is not known.

Since molten germanium is a metallic liquid where free electrons are responsible for the electrical and thermal conductivities, one can use the Wiedemann-Franz-Lorenz law to relate the thermal conductivity with the electric resistivity:

$$\frac{\kappa_{liq} r_{liq}}{T} = \frac{\pi^2 k^2}{3e^2} \equiv L_o = 2.45 \times 10^{-8} \quad W\Omega K^{-2}, \tag{11}$$

where k is the Boltzman constant and e is the electron charge. The constant $L_o = \pi^2 k^2 / 3e^2$ is the Lorenz number whose validity was experimentally confirmed with high accuracy by Busch et al.[26].

Using the Eq.s (10) and (11), one can obtain the following expression for the thermal conductivity of molten germanium:

$$\kappa_{liq}(T) = 49.43 + 2.90 \times 10^{-2} (T-1211.3) \quad W\,m^{-1}\,K^{-1}, \quad (1211.3 \sim 1380\ K) \tag{12}$$

and **Fig. 8** compares our result with two reference data available in the literature[22]. In this figure, the data by CINDA was obtained by converting the Glazov's electrical resistivity data (see **Fig. 7**) using the Wiedemann-Franz-Lorenz law. Only the Filippov's two data points were obtained through direct measurement of thermal conductivity. In **Fig. 8** we can observe that the choice of $r_{e,liq}(T_m) = 60\ \mu\Omega cm$ as a reference point to calibrated our resistivity data was a reasonable one since it converts to thermal conductivity at melting point which agrees closely with other data. In contrast to other two reference data, our work shows increasing trend of thermal conductivity as the temperature increases. The sample rotation technique used in this work is very sensitive in detecting relative changes of resistivity as a function of temperature. Also, according to CINDA's report, except molten germanium, other elements in Group IVA such as tin, lead, and silicon showed thermal conductivities which increased with increased temperature.

DISCUSSION

In this paper, we have reported for the first time various thermophysical properties of molten germanium using various non-contact diagnostic techniques which have been developed for the high temperature electrostatic levitator. The properties include the density, the thermal expansivity, the hemispherical total emissivity, the temperature dependence of constant pressure specific heat capacity, the surface tension, and the temperature dependence of electrical resistivity. The resistivity data was translated into the thermal conductivity using the Wiedemann-Franz-Lorenz law.

It was pointed out that the present technique measures the ratio c_{pl}/ε_T, rather than independent measurement of ε_T and c_{pl}. Therefore, only when valid c_{pl} at the melting temperature is available, ε_T can be determined with certainty.

We are surprised to see that our surface tension result smaller than the reference values as much as 3 ~ 6 %, although our germanium drop must have cleaner surface. We are planning to repeat this experiment in a near future. Also, it is worth pointing out that the present approach is not an adequate means of measuring the viscosity which is lower than ~ 1 mPascal·sec.

The electrical resistivity measuring technique is a new addition to our HTESL. At this point, it measures only relative changes of electrical resistivity although absolute measurement may be made possible in the future. Detailed description of this technique is beyond the scope of this paper, and it will be published elsewhere.

ACKNOWLEDGMENTS

The authors would like to thank Mr. Daniel Barber and Dr. Paul-Francois Paradis for various assistance in this work. This work was carried out at the Jet Propulsion Laboratory, California Institute of Technology, under contract with the National Aeronautical and Space Administration.

REFERENCES

1. W. K. Rhim, S. K. Chung, D. Barber, K. F. Man, G. Gutt, A. Rulison, and R. E. Spjut, Rev. Sci. Instrum. 64: 2961 (1993).

2. W. K. Rhim, S. K. Chung, A. J. Rulison, and R. E. Spjut, Int. J. Thermophysics, 18, 459, 1997

3. Sang K. Chung, David Thiessen, Yong J. Kim and Won-Kyu Rhim, Rev. Sci. Instrum. in press.

4. W. K. Rhim, K. Ohsaka, R. E. Spjut, Rev. Sci. Instrum. (submitted)

5. J. W. S. Rayleigh, Phil. Mag. 14: 184, (1882).

6. J. Q. Feng and K. V. Beard, Proc. R. Soc. Lond. A. 430: 133, (1990).

7. L. -D. Lucas: Liquid Density Measurements from Techniques of Metals Research IV (2), R. A. Rapp, ed., p. 219, Interscience Publishers, New York, 1970

8. Khilya, Ivaschchenko, and Eremenko, A. N. Ykr. SSR, Fis. Khim. Pov. Yavl. v Raspl., 149,1971

9. Tavadse, Khantadse, and Tsertsvadse, Vopr. Metalloved. i Korros. Met., Isdat. Metsniereba, Tiflis, 1968

10. T. Iida and R. I. L. Guthrie, The Physical Properties of Liquid Metals (Clarendon press, Oxford, 1988), p. 71.

11 A. J. Rulison and W. K. Rhim, Metallurgical and Materials Trans. B, 26B: 503 (1995).

12. O. Kubaschewski and C. B. Alcock, Metallurgical Chemistry (5th Edn, revised and enlarged). Pergamon Press, Oxford, 1979, p. 336 (Table C1)
13. L. P. Filippov, Int. J. Heat Transfer 16, 865-885, 1973.
14. R. K. Crouch, A. L. Fripp, W. J. Debnam, R. E. Taylor, and H. Groot, "Thermophysical Properties of germanium for thermal analysis of growth from the melt" Materials. Res. Soc. Sympo. on 'Materials Processing in the Reduced Gravity Environment of Space', [G. E. Rindone, Ed.], vol. 9 675-663, 1982
15. E. Takasuka, E. Tokizaki, K. Terashima and S. Kimura, "Spectral Emissivity of Liquid Germanium and Liquid Silicon", Proc. Fourth Asian Thermophysical Properties Conference, Tokyo, September 1995, p77
16. B. C. Allen, Liquid Metals: Chemistry and Phys. (ed. S. Z. Beer). Marcel Dekker, New York, p. 186 (Table 5), 1972
17. Y. Takamura, T. Aoyama, and K. Kuribayashi, "Containerless Solidification of Si-Ge Semiconductor Alloys by Electromagnetic Levitation", Proc. Spacebound 97 begins and the 9th Int. Sympo. on Exp. Methods for Micro-g Materials Science, Montreal, Canada, May 11~14, 1997
18. H. Lamb: Hydrodynamics, 6th ed., Cambridge University Press, 473-639, 1932.
19. V. M. Glazov, S. N. Chizhevskaya, and N. N. Glagoleva, Liquid Semiconductors (Plenum press, New York, 1969), p. 61.
20. V. F. Brekhovskikh, Progress in Heat Transfer (P. K. Konakov ed.), Consultants Bureau, New York 1966, pp. 145-150.
21. S. A. Nasar and I. Boldea, Electric Machines (Steady State Operation), Hemisphere Publishing Corporation 1990
22. P. L. Alger, Nature of Induction Machine, Gordon and Breach Science Publishers 1965
23. W. K. Rhim and T. Ishikawa, "Drop Rotation in the High Temperature Electrostatic Levitator for Noncontact Measurement of Electrical Resistivity", (to be published)
24. R. Keyes, Phys. Rev. 84, 367, 1951
25. C. Domenicali, J. Appl. Phys. 28, 749, 1957
26. G. Bush, H. -J. Guntherodt, W. Haller, and P. Wyssmann, Phys. Lett. 43A, 225, 1973.

Table I. Mass densities of molten germanium are compared.

	$\rho_{liq.}(T_m)$ x10^3 Kg/m^3	$d\rho_{liq.}/dT$ x10^{-1} Kg/Tm^3
Lucas [7]	5.49	- 4.9
Khilya et al. [8]	5.655	- 6.1
Tavadse et al. [9]	5.598	- 6.25
Present work	5.67	- 5.42

FIGURE CAPTION

Fig. 1. Schematic diagram of the electrode assembly used in the HTESL.

Fig.2. A typical cooling profile of molten germanium drops as they undergo purely radiative cooling process.

Fig. 3. Density of molten germanium as a function of temperature.

Fig. 4. c_{pl}/ε_T vs. temperature of molten germanium as calculated from data shown in Fig. 1.

Fig. 5. $c_p(T)$ vs. temperature calculated from result shown in Fig. 4 assuming $\varepsilon_T(T) = \varepsilon_T(T_m) = 0.17$.

Fig. 6. Surface tension $\sigma(T)$ of molten germanium as a function of temperature.

Fig. 7. Electrical resistivity of molten germanium as a function of temperature.

Fig. 8. Thermal conductivity of molten germanium obtained from Eq. (10) using the Wiedemann-Franz-Lorenz law along with existing reference data.

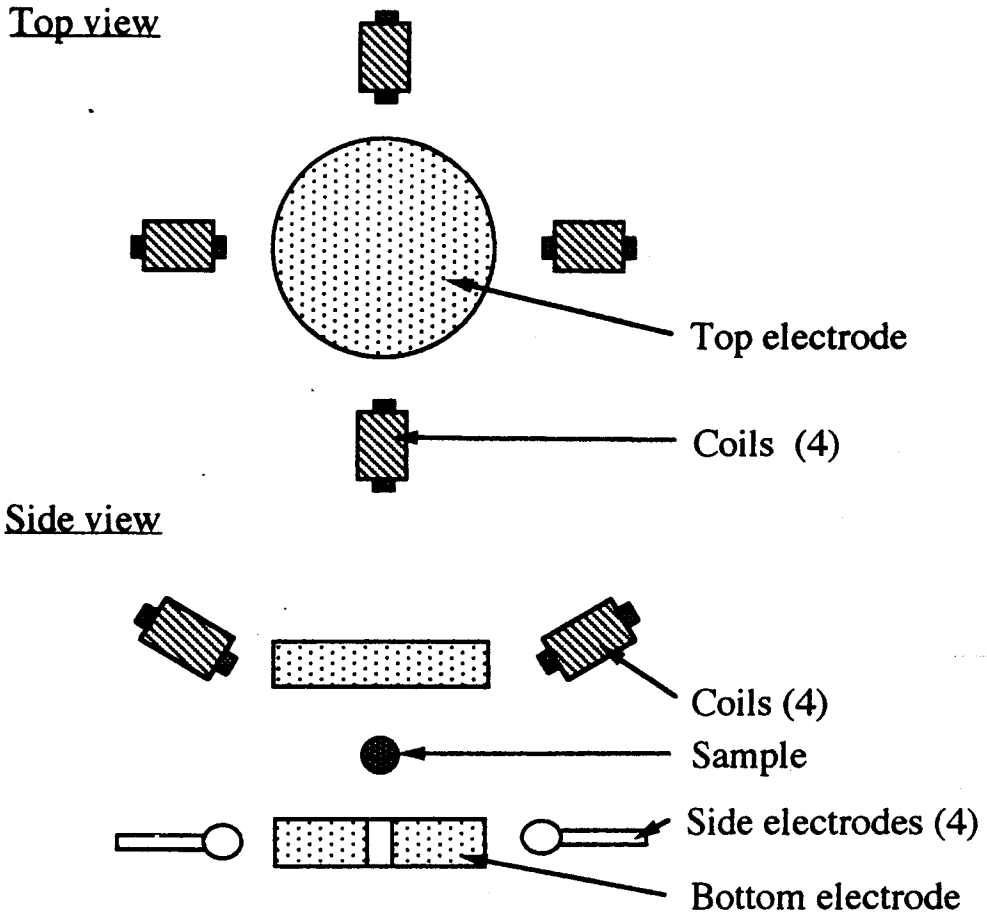
Top view
Top electrode
Coils (4)
Side view
Coils (4)
Sample
Side electrodes (4)
Bottom electrode

Fig-1

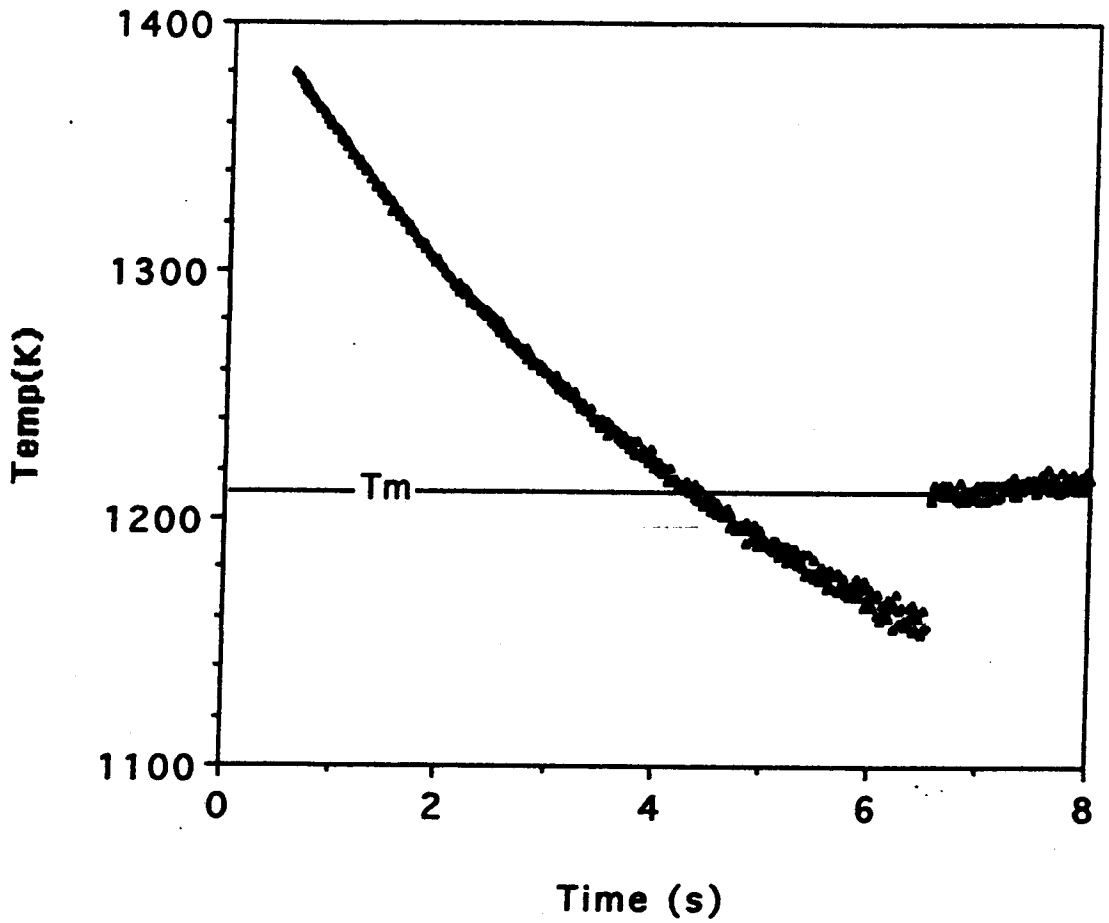

Fig-2

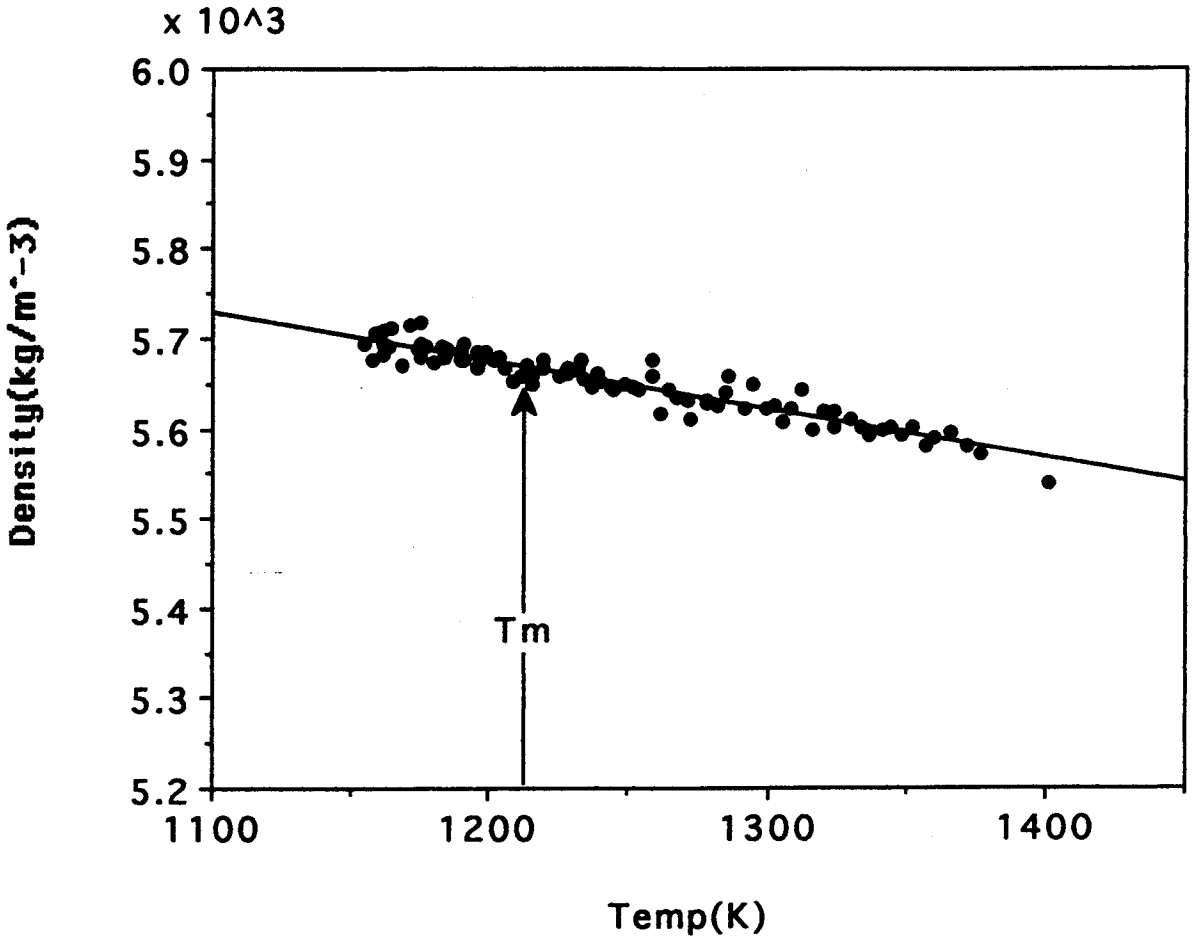
x 10^3
6.0
5.9
5.8
5.7
5.6
5.5
5.4
5.3
5.2
Density(kg/m^-3)
Tm
1100
1200
1300
1400
Temp(K)

Fig-3

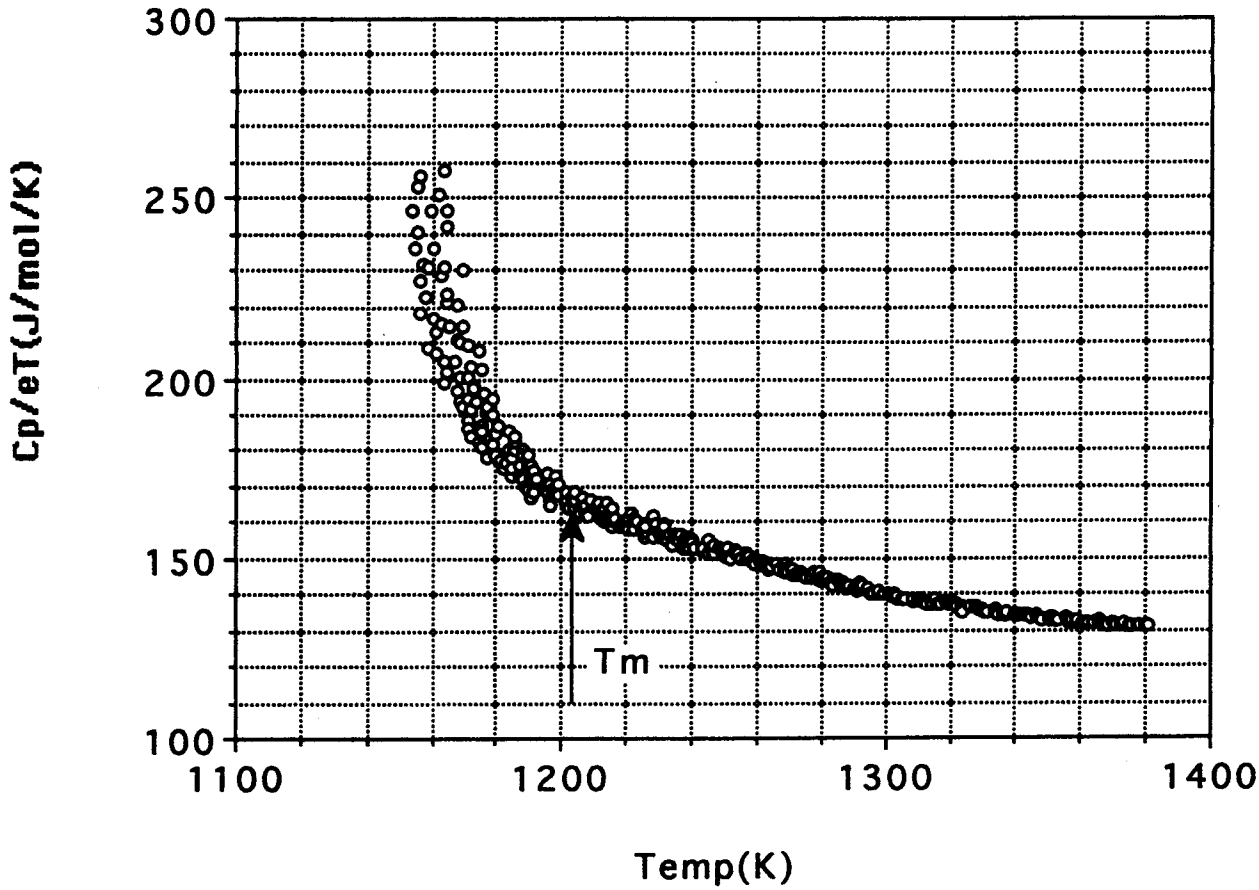

Fig-4

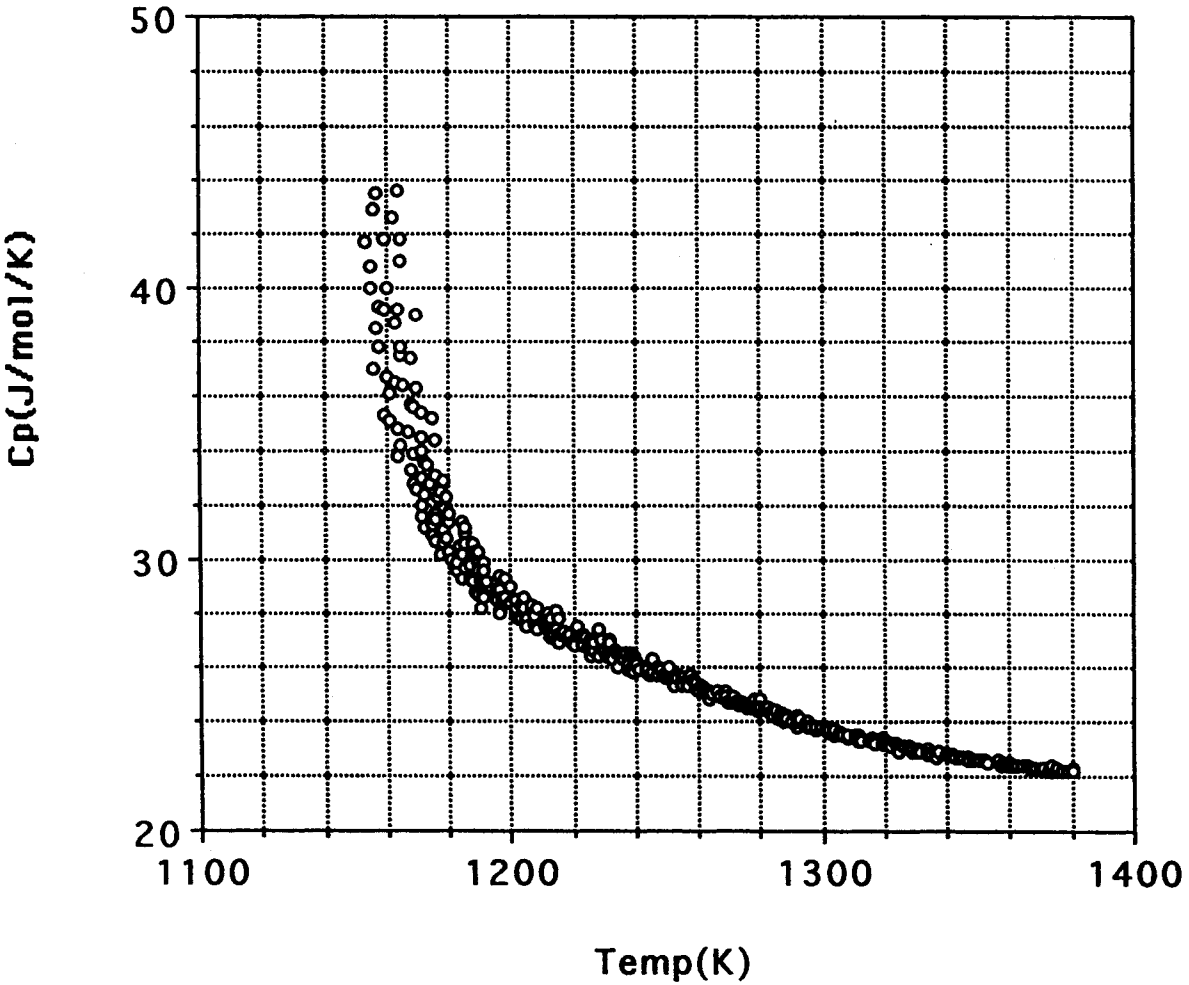

Fig-5

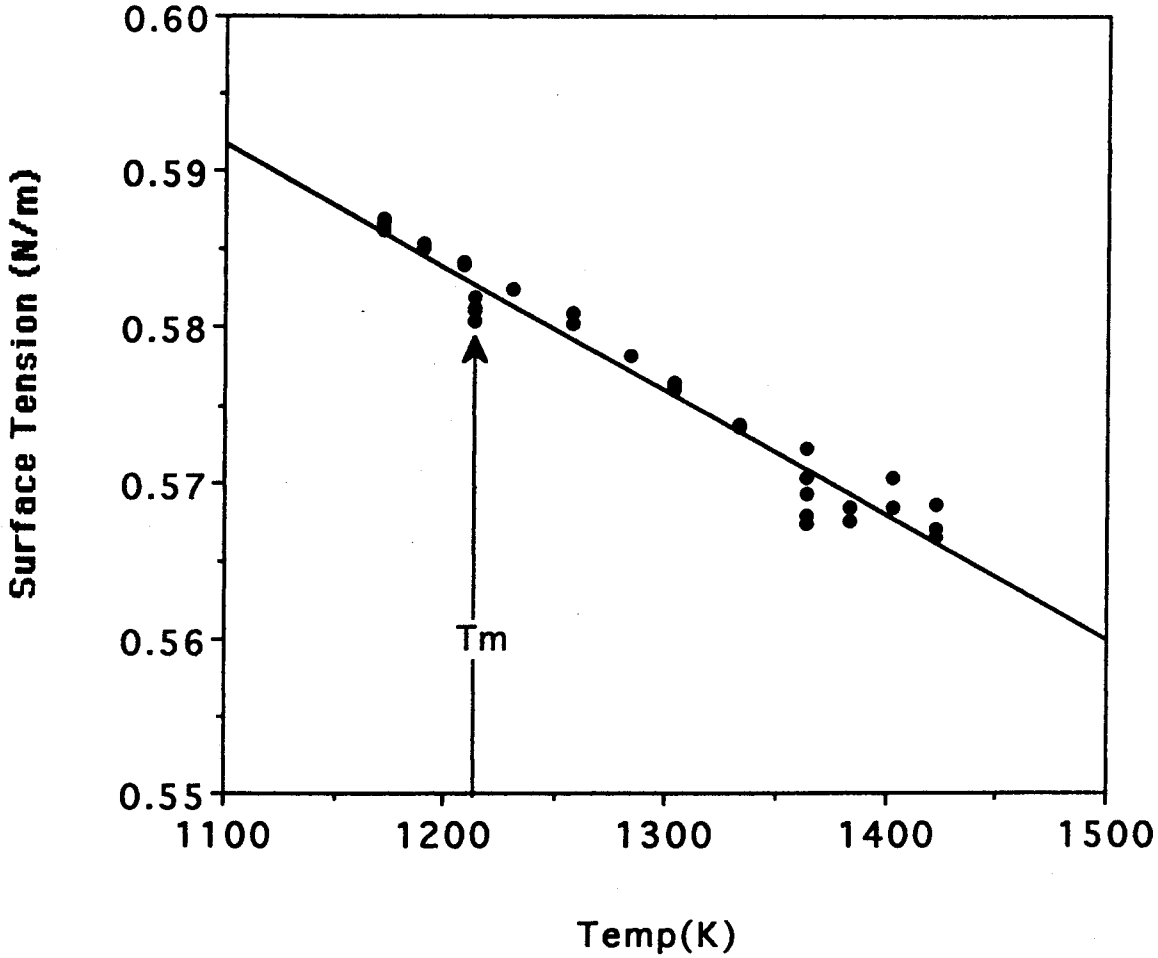
0.60
0.59
0.58
0.57
0.56
0.55
Surface Tension (N/m)
Tm
1100
1200
1300
1400
1500
Temp(K)

Fig-6

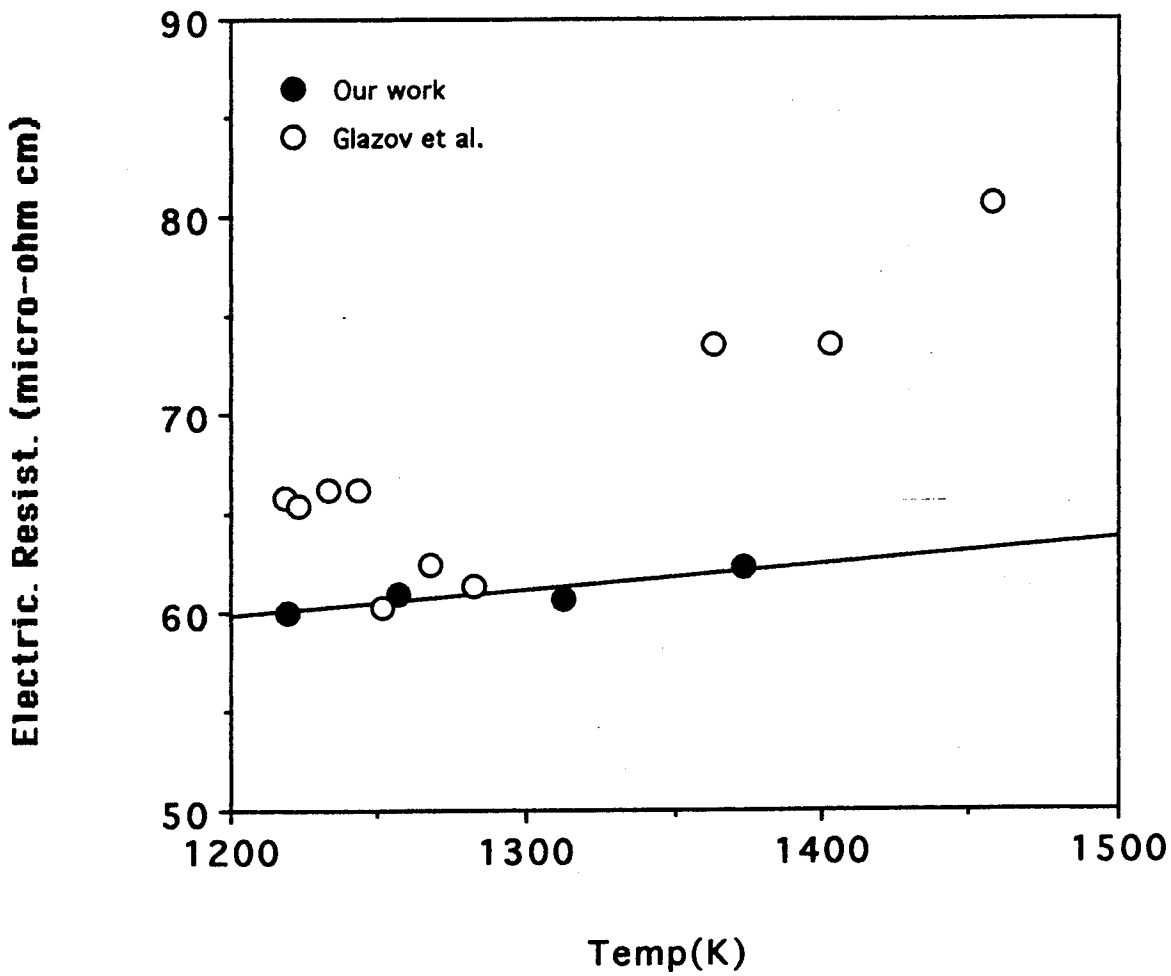
Electric. Resist. (micro-ohm cm)
90
80
70
60
50
Our work
Glazov et al.
1200
1300
1400
1500
Temp(K)

Fig-7

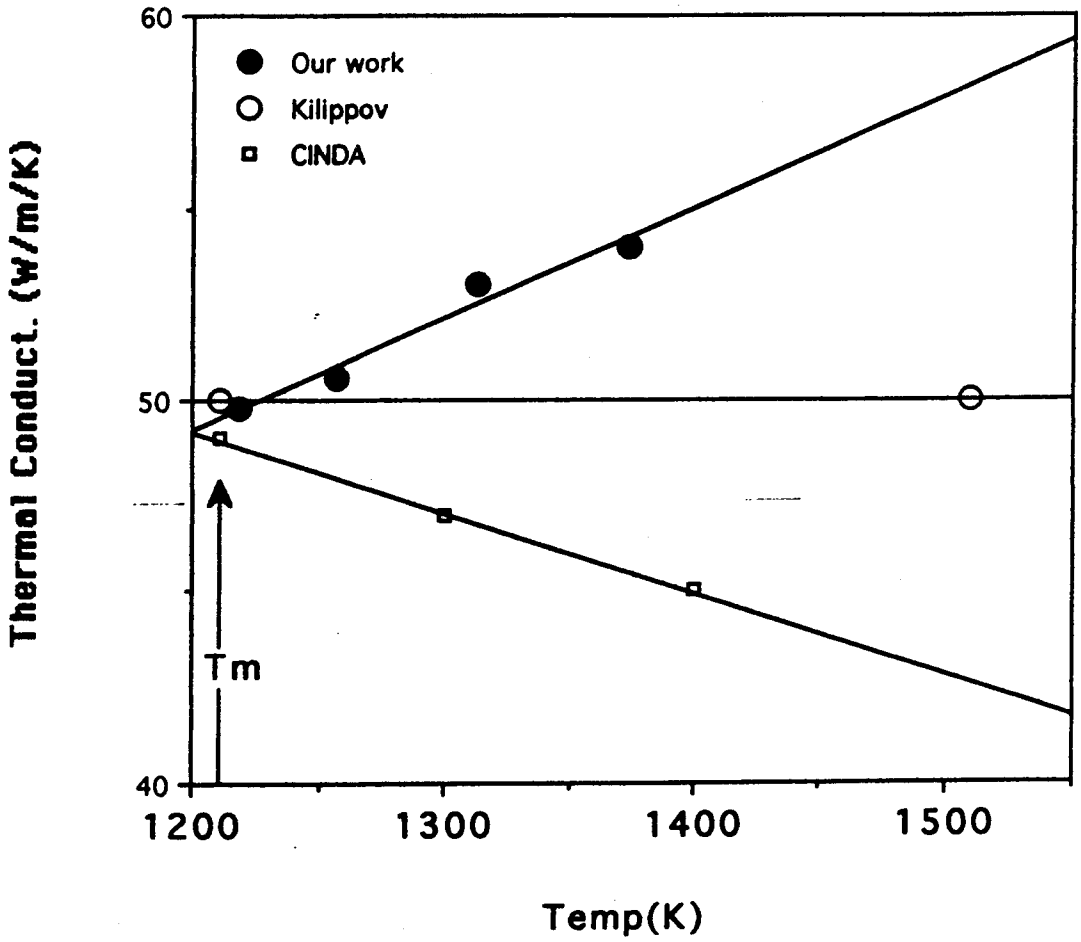
60
50
40
Our work
Kilippov
CINDA
Tm
1200
1300
1400
1500
Thermal Conduct. (W/m/K)
Temp(K)

Fig-8